

Dalton Transactions

An international journal of inorganic chemistry

Accepted Manuscript

This article can be cited before page numbers have been issued, to do this please use: J. E. Expósito, G. Aullón, M. Bardaji, J. A. Miguel and P. Espinet, *Dalton Trans.*, 2020, DOI: 10.1039/D0DT02494E.



This is an Accepted Manuscript, which has been through the Royal Society of Chemistry peer review process and has been accepted for publication.

Accepted Manuscripts are published online shortly after acceptance, before technical editing, formatting and proof reading. Using this free service, authors can make their results available to the community, in citable form, before we publish the edited article. We will replace this Accepted Manuscript with the edited and formatted Advance Article as soon as it is available.

You can find more information about Accepted Manuscripts in the [Information for Authors](#).

Please note that technical editing may introduce minor changes to the text and/or graphics, which may alter content. The journal's standard [Terms & Conditions](#) and the [Ethical guidelines](#) still apply. In no event shall the Royal Society of Chemistry be held responsible for any errors or omissions in this Accepted Manuscript or any consequences arising from the use of any information it contains.

ARTICLE

Fluorescent perylenylpyridine complexes: an experimental and theoretical study[†]J. Emilio Expósito,^a Gabriel Aullón,^b Manuel Bardají,^a Jesús A. Miguel,^{*a} and Pablo Espinet^{*a}Received 00th January 20xx,
Accepted 00th January 20xx

DOI: 10.1039/x0xx00000x

The perylene derivative 2-(3-perylenyl)-4-methylpyridine (HPerPy) was prepared and used to synthesize [Ag(HPerPy)(PPh₃)(OCIO₃)], with the perylene ligand bonded to the metal centre only by the pyridine nitrogen. Treatment of HPerPy with [Pd(OAc)₂] in methanol or acetic acid led to the acetate bridged dimers (μ-OOCCH₃)₂[Pd(PerPy)]₂, six-membered or five-membered cyclized at the perylenyl fragment. Substitution reactions afforded mononuclear compounds [Pd(PerPy)(acac)] (six-member or five-member cyclized) and [Pd(PerPy)(S₂COMe)] (six-member or five-member cyclized). Reaction of HPerPy with a platinum(II) fragment led to the five-membered cyclometallated Pt(II) complex [Pt(PerPy)(acac)]. Oxidative addition with MeI gave the corresponding cyclometallated Pt(IV) compound [Pt(PerPy)(acac)MeI]. X-ray single crystal studies of compounds [Ag(HPerPy)(PPh₃)(OCIO₃)], (μ-OOCCH₃)₂[Pd(PerPy)]₂-five-membered, [Pd(PerPy)(acac)]-six-membered, [Pd(PerPy)(S₂COMe)]-five-membered, [Pt(PerPy)(acac)]-five-membered, and [Pt(PerPy)(acac)MeI]-five-membered confirmed the proposed structures. The UV-Vis spectra show one intense absorption with vibronic coupling in the visible region with maxima in the range 448-519 nm. DFT calculations were carried out for the absorption spectra of the HPerPy molecule and representative complexes [M(PerPy)(acac)] (M: Pd, Pt; five and six-membered isomers) and [Pt(PerPy)(acac)MeI], showing that the lowest energy most intense transition in the complexes corresponds to the HOMO → LUMO transition in the perylene moiety, although affected by the metallacycle size and the metal nature. All the compounds are fluorescent in solution, due to the perylene fragment. The emission spectra display maxima in the range 468-549 nm, with quantum yields from 1.1 to 82%. The attenuation of the intensity of fluorescence by the presence of heavy atoms and the formation of metallacycles has been experimentally determined and sequenced.

Introduction

Perylene compounds are chromophores with excellent chemical and photochemical stability, and exhibit strong absorption of visible light and high fluorescence quantum yields. The emissive excited states of these compounds are mainly centred at the perylene core. Due to these exceptional properties, they have been employed as industrial pigments,¹ in several electronic and optical applications,² as liquid crystals,³ for highly fluorescent J-aggregates⁴ and in thin films with a good molecular ordering.⁵

Because of the presence of non-equivalent metallation positions, the cyclometallation of N-donor ligands containing fused rings raises the question of regioselectivity.⁶ The

corresponding Pd(II) compounds, very used in metal mediated organic synthesis and in homogenous catalysis, exhibit weak or non-luminescence at room temperature due to the presence of low-lying metal-centered excited states that deactivate the potentially luminescent MLCT and IL levels.⁷ Therefore, luminescent room temperature palladacycles are comparatively scarce.⁸ In contrast, the use of 2-arylpyridines has been particularly successful, because they yield coloured complexes with high phosphorescent emission efficiency, most often for Pt(II)⁹ and more scarcely for Pt(IV).¹⁰ The use of late transition metals exhibiting large spin-orbit coupling (SOC) in organic chromophores allows for facile tuning of the excited states, and facilitates a rapid singlet to triplet intersystem crossing (ISC), the population of the triplet state, and finally the triplet to singlet radiative transition (phosphorescence). The emissive excited states of these complexes are usually ³IL (phenyl to pyridine) or ³MLCT, (metal to pyridine) triplet states.

Changing the substituents in the aromatic core can significantly modify the solubility, electronic and optical properties of perylenes. Besides, metal centres and their ancillary ligands allow for the modification of the optoelectronic properties, and provide therefore a good opportunity to build new functional and structural motifs, significantly widening the diversity of photofunctional systems available.¹¹ For this purpose, a simple strategy to modulate

^a IU CINQUIMA/Química Inorgánica, Facultad de Ciencias, Universidad de Valladolid, 47071 Valladolid (Spain).

^b Departament de Química Inorgànica, Universitat de Barcelona, Martí i Franquès 1-11, E-08028 Barcelona, (Spain).

[†] Electronic Supplementary Information (ESI) available: NMR spectra, study of reaction conditions to obtain complexes **3** and **4**; crystallographic information and X-ray packings; absorption and emission spectra of complexes in different solvents; emission spectra at 77K and in the solid state; computational data: relative free energies, calculated absorption parameters, molecular orbitals and calculated electronic spectra in chloroform; lifetime measurements. CCDC reference numbers 2015584-2015589 for **2**, **4**, **5**, **8**, **9**, and **10**. For ESI and crystallographic data in CIF or other electronic format see DOI: 10.1039/b000000x.

the properties of perylene systems is the functionalization of the perylene core in the desired position with a functional donor group for metallic fragments. Using this approach, we have reported before highly fluorescent perylene derivatives with Au, Pd or Pt complex fragments attached to perylene through a tetrafluorophenyl linker,¹² or complexes with an isocyanide group acting as the connector between Au, Pd, Cr, Mo, W complex fragments and the perylene chromophore.¹³ In both cases, the perylene electron density is weakly influenced by the substituents in the ring and by the metal fragments. In contrast, ethynyl-substituted perylene or perylene monoimide Pt^{II} complexes are not emissive, but readily sensitize ¹O₂ due to the population of the perylene centred triplet excited state.^{14,15} Finally, [Ru(bpy)₂(ab-PBI)][PF₆]₂ and [Cp*Ir(ab-PBI)Cl]PF₆ (ab-PBI = azabenzannulated perylene bisimide) not only quench the fluorescence, but show NIR phosphorescence in solution at room temperature.¹⁶

A second metal based approach to modify the properties of perylenes is the incorporation of a moiety with the metal centre σ -bonded directly to the perylene core. In this context, we have reported Pt^{II} complexes of perylene and perylene monoimide where the metal coordination has only a moderate quenching effect and the complexes still display intense fluorescent emissions.¹⁷ A similar result was reported by others for perylene diimide Pd^{II} compounds.¹⁸ However, Pt^{II} complexes σ -bonded to perylene diimides are able to produce partial or total fluorescence quench by facilitating the intersystem crossing to populate the triplet excited state.¹⁹

The combination of both strategies was achieved using a coordinating ligand able to induce cyclometallation (perylene imine). This afforded cyclopalladated or cycloplatinated complexes with very modest quantum yields (in the range 0.01–0.13 for Pd^{II}, and < 0.01 for Pt^{II}). Interestingly, the quantum yields were much higher for Pt^{IV} (up to 0.29).^{6a,6b,20} The fluorescence was associated based in the perylene moiety, and no phosphorescence was observed. In addition, five or six-membered palladacycles were isolated.

Here we report a set of new complexes based in the ligand 2-(3-perylenyl)-4-methylpyridine, and the study of their selective metallation and their optical properties. This pyridine ligand can initially coordinate to a metal, and then induce metallation via C-H activation of the perylene core at positions 2 (*ortho*; five-membered cycle) or 4 (*peri*; six-membered cycle), as shown in Figure 1. The Me substituent enhances the solubility of the compounds, and facilitates observations in NMR studies.

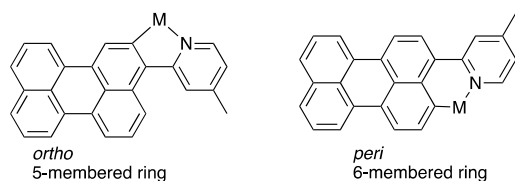


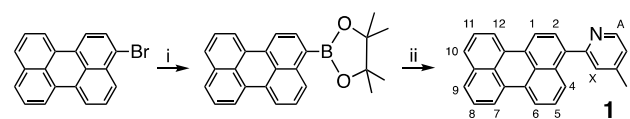
Fig. 1 Metallated alternative structures of the new perylene ligand.

This ligand can bring about fluorescence due to the perylene core, or phosphorescence induced by pyridine cyclometallated compounds. First, a non-metallated Ag^I derivative, only coordinated through pyridine was studied to see the effect of a metal centre as a simple Lewis acid. Then, Pd^{II}, Pt^{II} and Pt^{IV} complexes were prepared to test the effect of cyclometallation, as well as the effect of the Pt oxidation state. Finally, a thorough study of the optical properties was carried out, including theoretical calculations in order to support the transition assignments.

Results and discussion

Syntheses and characterization

The 3-perylene boronic ester was prepared by reaction of 3-bromoperylene with bis(pinacolato)diboron in 1,4-dioxane catalysed by [PdCl₂(dppf)] (dppf = 1,1'-bis(disphenylphosphino)ferrocene).²¹ A Suzuki coupling reaction of this boronic ester with 2-bromo-4-methylpyridine, catalysed by [PdCl₂(dppf)], led to 2-(3-perylenyl)-4-methylpyridine HPerPy **1** (Scheme 1). The closely related Stille coupling of 3-bromoperylene with pyridyl stannane to prepare 2-(3-perylenyl)pyridine had been reported previously.²² Compound **1** is a yellow solid moderately soluble in organic solvents. Its ¹H NMR spectrum displays the corresponding perylene protons and an AMX spin system plus a methyl singlet for the methylpyridine fragment.

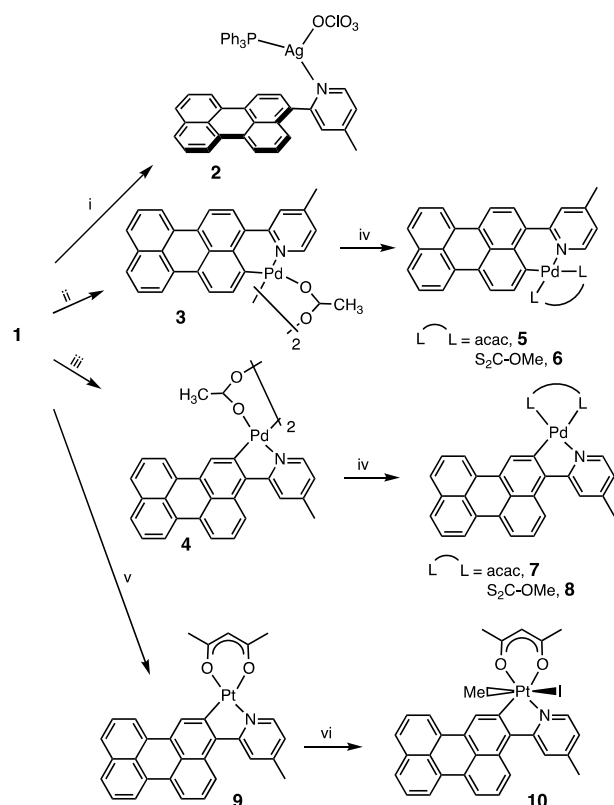


Scheme 1 i) B₂(pin)₂, ii) THF, CsF, PdCl₂(dppf), and 2-bromo-methylpyridine. Number/letter key for H atoms.

The syntheses of Ag, Pd and Pt compounds are shown in Scheme 2. The treatment of HPerPy with a phosphine silver(I) compound afforded compound **2** as a yellow solid. The structure was clearly confirmed by a single-crystal X-ray study. Reactions of HPerPy with palladium acetate in toluene yielded mixtures of the five and six-membered palladacycles, which could not be separated. Looking for chemoselective syntheses (see Table S1 in the ESI[†]), the best reaction conditions were the following: the reaction in methanol for 15 h at 25 °C gave compound **3**. The ¹H NMR spectrum of **3** showed it to be a pure isomer, the *anti*-(6+6) isomer (C₂ symmetry) in an open book (V-shaped) structure. On the other hand the reaction carried out in acetic acid, 6 h at 70 °C, produced a product labelled **4**. The ¹H NMR spectrum of **4** revealed it to be a mixture of the 5+5 (66%), and 5+6 (34%) cyclometallated dimers. They could not be separated but the structure of a single crystal, which turned out to be the predominant (5+5) isomer, could be confirmed by crystallographic studies.

Further treatment of **3** or **4** with acetylacetonate, or with CS₂

in basic media, afforded the corresponding mononuclear acetylacetonate or xanthate palladacycles **5-6** (six-membered) and **7-8** (five-membered). After workup, compounds **7-8** were shown to be isomerically pure. Compounds **5-6** are red solids while **7-8** are very dark in colour. The ^1H NMR spectra displayed a doublet for H^1 for compounds **5-6**, and a singlet for **7-8**, which supports the existence of six or, respectively, five-membered cycles as depicted. The molecular structures of compounds **5** and **8** were assessed by crystallographic studies.



Scheme 2 (i) $[\text{Ag}(\text{PPh}_3)(\text{OCIO}_3)]$, CH_2Cl_2 , 25 °C, 4 h; (ii) $\text{Pd}(\text{OAc})_2$, methanol, 25 °C, 15 h; (iii) $\text{Pd}(\text{OAc})_2$, CH_3COOH , 70 °C, 6 h; (iv) Hacac, KOH + MeOH, CH_2Cl_2 , 25 °C, 24 h (**5**, **7**); CS_2 , KOH + MeOH, CH_2Cl_2 , 25 °C, 24 h (**6**, **8**); (v) K_2PtCl_4 , 2-ethoxyethanol/water, reflux, 22 h; $\text{TI}(\text{acac})$, CH_2Cl_2 , 25 °C, 5 h; (vi) MeI, acetone, 25 °C, 48 h. The dimers of **4** are a mixture of 5+5 and 5+6 isomers, with their syn and anti (dominant) forms.

The reaction of **1** with K_2PtCl_4 at reflux afforded a poorly soluble chloro-bridged dimer, which could not be purified, but further reaction with $\text{TI}(\text{acac})$ led to the five-membered orthoplatinated compound **9**, and oxidative addition with MeI produced the platinum(IV) compound **10**. Compounds **9** and **10** are orange solids. The ^1H NMR spectra of the square-planar **9** and the octahedral **10** show, as expected, a singlet with ^{195}Pt satellites (orthoplatinacycle) for H^1 , and two non-equivalent methyl groups for the acetylacetonate group. A NOESY experiment supports the assignments of H^1 . Comparing the ^1H NMR parameters of **9** versus **10**, a decrease in value of $^3J_{\text{Pt-H}}$ and a slight upfield shift of all the protons is observed for **10**, consistent with its higher Pt oxidation state. The molecular

structures of **9** and **10** were confirmed by single-crystal X-ray diffraction studies.

View Article Online
DOI: 10.1039/D0DT02494E

Crystal structures

The single-crystal X-ray crystal structure of **2** (Fig. 2) confirms the proposal in Scheme 2. Selected bond lengths and angles are given as figure caption. The Ag^{I} centre is coordinated only to the pyridine nitrogen, the phosphine and one oxygen of the perchlorate anion. It is the only structure in this work without metallation, which is useful for comparison in the photophysical studies. The silver centre displays a highly distorted trigonal geometry, with a large N1-Ag-P1 angle of $159.59(7)^\circ$, smaller P1-Ag-O1 of $120.9(2)^\circ$, and the smallest N1-Ag-O of $79.6(2)^\circ$. Note the large Ag-O1-Cl angle of $135.3(7)^\circ$ due to intermolecular hydrogen bonds O1-H25 , O4-H26A and O4-H28 of 2.465, 2.353 and 2.483 Å, respectively. The perylene fragment is planar with a dihedral angle of 1.57° , but it shows a large dihedral angle of 55.46° with pyridine. There is no π - π stacking between perylenyl rings.

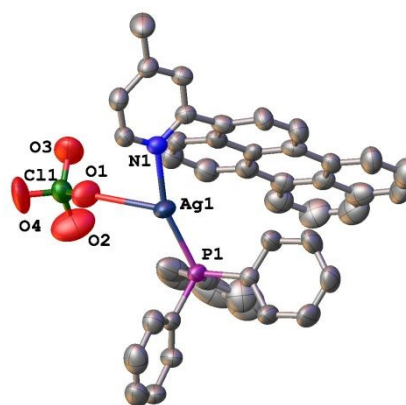


Fig. 2 Molecular structure of complex **2**. H atoms are omitted for clarity. Relevant bond lengths (Å) and angles ($^\circ$) are: Ag-P1 2.3719(9); Ag-N1 2.222(3); Ag-O1 2.614(9); N1-Ag-P1 $159.59(7)^\circ$; P1-Ag-O1 $120.9(2)^\circ$; N1-Ag-O1A $79.6(2)^\circ$; Ag-O1-Cl $135.3(7)^\circ$.

The single-crystal X-ray crystal structures of **4**, **5**, **8**, **9**, and **10** are shown in Fig. 3-4, and confirm the structures proposed in Scheme 2. Selected bond lengths and angles are given in Table 1. Compounds **4**, **5** and **8** (Pd), as well as **9** (Pt), display a distorted square-planar geometry for the M^{II} centre. Compound **10** shows a distorted octahedral coordination of the Pt^{IV} centre, where the chelate ligands are equatorial and the iodide and methyl groups are axial. The molecular structure of compound **4** confirms a dinuclear molecule of the *anti*-(5+5) isomer, with C_2 symmetry. A Pd-Pd distance of 2.8614(4) Å is observed, typical for these acetate-bridged dinuclear compounds. Both Pd(PerPy) units form an angle of 22.61° measured between perylenyl fragments. The Pt-O bond lengths in the acac complexes are slightly longer in Pt^{IV} (**10**) than in Pt^{II} (**9**), and reflect the dissimilar *trans* influences of N- and C-donors.²³ This is also observed for Pd-O and Pd-S in compounds **4**, **5** and **8**.

The structures of the palladium **4** and **8**, and platinum **9-10** compounds consist of a planar five-membered metallacycle, with

the average perylene plane almost coplanar with the coordination plane of metal: 3.80° (**4**), 18.16° (**8**), 8.33° (**9**) and 11.91° (equatorial plane of **10**). The perylene fragment is essentially planar: the two "naphthalene" moieties forming the perylene show a dihedral angle of 0.90° (**4** and **9**), and are more distorted for xanthate Pd^{II} **8** (9.06°) and Pt^{IV} **10** (5.60°). There is no π - π stacking of the perylenyl rings in compounds **8** (in this one the molecules are arranged in head-tail pairs) and **9**. Compounds **4** and **5** show partial π - π stacking between perylenyl rings, with distances 3.358 and 3.373 Å, respectively (see Fig. S14-S15 in the ESI[†]). Surprisingly, because octahedral Pt^{IV} is expected to have more steric hindrance than square-planar Pt^{II}, complex **10** shows partial π - π stacking between perylenyl rings, with 3.523 Å ring to ring distance (see Fig. S16 in the ESI[†]).

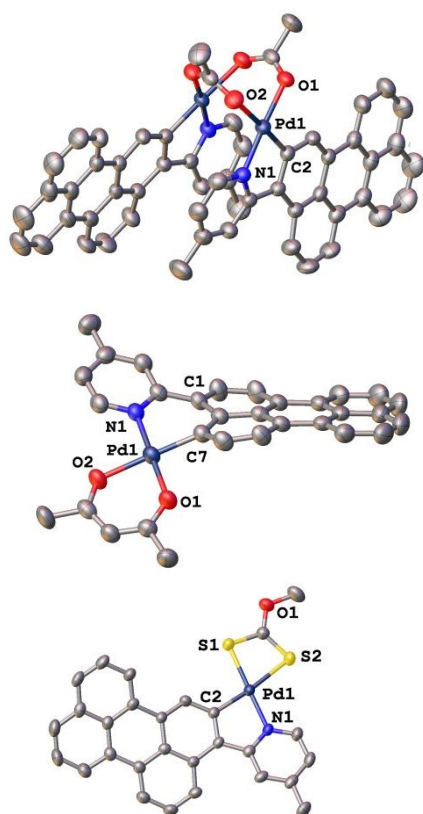


Fig. 3 Molecular structures of complexes **4** (above), **5** (middle), and **8** (below). H atoms are omitted for clarity.

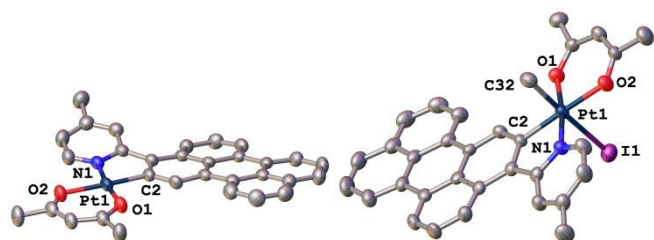


Fig. 4 Molecular structures of complexes **9** (left) and **10** (right). H atoms are omitted for clarity.

The Pd compound **5** and the Pt complex **9** are stoichiometrically related, but the six-membered metallacycle in **5** instead of a five-membered one in **9** forces relevant structural differences. First, the

six-membered palladacycle in **5** has an envelope conformation: N(1)–C(21)–C(1)–C(6)–C(7) are in a plane and the Pd atom is 0.781 Å out of this plane. Something similar was reported for imine perylene palladium complexes.^{6a,6b} In contrast, the five-membered platinacycle in **9** is planar. Furthermore, the perylene fragment in **5** is distorted from planarity as shown by a dihedral angle of 7.80° between the two "naphthalene" halves forming the perylene (this angle is only 0.90° for **9**). Finally, the average perylene plane forms an angle of 42.69° with the coordination plane of palladium in **5**, in contrast to 8.33° found in compound **9**.

Table 1. Selected Interatomic Distances (Å) and Angles (°) for the complexes **4**, **5**, **8**, **9** and **10**.

Magnitude (Å or °)	4 (Pd)	5 (Pd)	8 (Pd)	9 (Pt)	10 (Pt)
M–C(2)/(C(7))	1.959(2)	1.966(4)	1.984(4)	1.962(4)	1.983(4)
M–N(1)	1.986(2)	2.005(3)	2.030(3)	1.981(3)	1.994(4)
M–O(1)	2.0377(18)	2.038(3)		2.005(3)	2.024(3)
M–O(2)	2.1868(18)	2.098(3)		2.090(2)	2.122(3)
Pt–C(32)					2.056(6)
Pt–I					2.7920(5)
Pd–S(1)			2.3113(11)		
Pd–S(2)			2.4431(12)		
Pd–Pd	2.8614(4)				
N(1)–M–C(2)/(C(7))	80.25(9)	89.88(15)	80.13(15)	80.67(14)	80.39(17)
O(1)–M–O(2)	86.67(7)	89.56(10)		91.15(10)	91.53(13)
N(1)–M–O(2)	97.34(8)	89.56(10)		94.88(11)	94.00(14)
C2/(C7)–M–O(1)	95.74(9)	89.95(14)		93.33(13)	93.93(16)

Photophysical Studies

UV–Vis absorption spectra. The UV–Vis absorption and emission data of dilute chloroform solution ($\sim 10^{-5}$ M) of the 2-(3-perylenyl)-4-methylpyridine HPerPy **1** and its silver, palladium and platinum complexes are summarized in Table 2. The absorption spectrum of HPerPy is compared with those of its complexes (Fig. 5) to illustrate the influence of the metallic fragment on the photophysical properties of the perylenylpyridine system. Compound **4** was not studied because it is a mixture of two isomers.

All the spectra display a very intense band in the UV region at 250–300 nm, which is not shown in the figure. The visible absorption of the perylenylpyridine (Fig. 5A) is a band with the maximum at 448 nm, red-shifted by about 460 cm^{-1} compared to perylene. In addition, a vibronic structure covering the range 350–480 nm is observed, with a vibrational spacing of about 1200 cm^{-1} , related to the stretching $\nu(\text{C}=\text{C})$ frequency of the polyaromatic system and with increasing intensity of the vibronic bands for the higher λ value.

The visible absorption spectrum of the silver compound **2** does not show any change compared to HPerPy, because it is only N-coordinated (Fig. 5A). In contrast, palladium and platinum spectra are red-shifted compared to perylene, due to electronic density delocalization of perylene into the metals, assisted by the formation of planar metallacycles.

Table 2 UV–Visible absorption and emission data for perylenylpyridine (**1**) and its complexes **2–3** and **5–10**, in chloroform at 298 K.

Comp.	λ (nm) ($10^3 \epsilon$)/dm ³ mol ⁻¹ cm ⁻¹	λ_{ex} /nm	λ_{em} /nm	Φ_f (%) ^a	τ^b /ns
HPerPy	256(31.1), 401(12.2), 422(26.2), 448(31.9)	424, 448	468, 490	82	3.74 (99.1), 0.51 (0.9)
2	256(47.3), 405(12.9), 424(25.4), 448(30.9)	425, 448	470, 491	78	3.76 (100)
3	238(70.7), 270(49.5), 352(13.7), 458(23.5), 484(46.2), 519(59.5)	470, 506	549	1.5 ^c	- ^d
5	270(31.1), 355(8.2), 458(12.4), 482(24.5), 516(30.8)	481, 514	547	47 ^c	1.6 (60), 0.023 (40)
6	263(51.8), 340(10.6), 456(14.5), 480(28.6), 512(36.3)	479, 511	545	5.5 ^c	0.034 (32.8), 0.28 (67.2)
7	246(39.2), 293(16.9), 451(12.6), 470(22.0), 500(26.0)	470, 499	522, 551	25 ^c	0.032(50.7), 0.042(49.3)
8	264(44.1), 300(19.5), 342(8.6), 455(14.0), 476(24.4), 506(29.3)	470, 504	535	2.7 ^c	0.10 (34), 0.16·10 ⁻³ (66)
9	265(50.0), 298(23.3), 417(15.1), 436(19.5), 483(28.4), 514(31.8)	455, 480	534	1.1 ^e	0.31 (88.4), 2.81 (11.6)
10	270(58.1), 449(16.8), 472(32.2), 502(37.9)	471, 501	526, 556	20	0.16 (87.6), 3.30 (12.4)

^a Quantum Yield. Relative to perylene in ethanol ($\Phi_f = 0.92$), and using an excitation wavelength of 434 nm. ^b Fluorescence lifetimes. Some decays were biexponential; the percentage of each component is shown in parentheses. ^c Determined in chloroform using Rhodamine B in ethanol ($\Phi_f = 0.70$) and using an excitation wavelength of 510 nm. ^d Not measurable due to low intensity. ^e Relative to Rhodamine 123 in ethanol ($\Phi_f = 0.96$) and using an excitation wavelength of 488 nm

The visible absorption spectra of the Pd^{II} compounds **3** and **5–8** (Fig. 5A) display a profile similar to that of the free ligand HPerPy (**1**), consisting of one absorption containing three bands due to vibronic coupling. In the complexes, this absorption is clearly red shifted (2000–3050 cm⁻¹) relative to **1**. It is tentatively assigned to a HOMO → LUMO transition in each complex, centred in the perylene ligand, and shows a small solvent dependence: 410 cm⁻¹ for **5** and 680 cm⁻¹ for **7**, when the solvent is changed from acetonitrile to toluene (see Fig. S17 in the ESI[†]). This will be discussed in more detail below, with the aid of TD-DFT calculations. Comparing the UV-Vis spectra of **5–6** (6-membered paladacycles) with **7–8** (5-membered palladacycles) in Figs. 5A and 5C, the latter show larger red shifts (230–620 cm⁻¹) and more intense bands. We found similar results in imine perylene palladacycles.^{6b}

As an exception, the visible absorption spectrum of the Pt^{II} compound **9** (Fig. 5B) displays two absorption bands with vibronic structure: one at 380–455 nm, and another at 465–535 nm, both with increasing intensity of the vibronic bands for higher λ values. We reported the same observation for imine perylene Pt^{II} compounds²⁰ where the lower energy absorption band was tentatively assigned to HOMO → LUMO transitions and the higher energy band to the platinum complexation effect. These bands show very little solvent dependence, less than 460 cm⁻¹, when the solvent changes from acetonitrile to toluene (see Fig. S18 in the ESI[†]). The absorption maximum is red shifted 100 nm in comparison with the related pyridine pyrene Pt^{II} compound (415 for pyrene vs 514 nm for **9**), as expected for the larger number of aromatic rings.²⁴ The origin of these bands is discussed below, with the TD-DFT calculations.

In summary, bathochromic shifts are observed for the absorption maxima (up to 3050 cm⁻¹) in the metallacycles from the HPerPy ligand, following the order: platinum(IV) and palladium(II) (5-member cycle) < platinum(II) < palladium(II) (6-member cycle). In contrast, the UV-Vis spectrum of HPerPy **1** remains unchanged after coordination to silver(I).

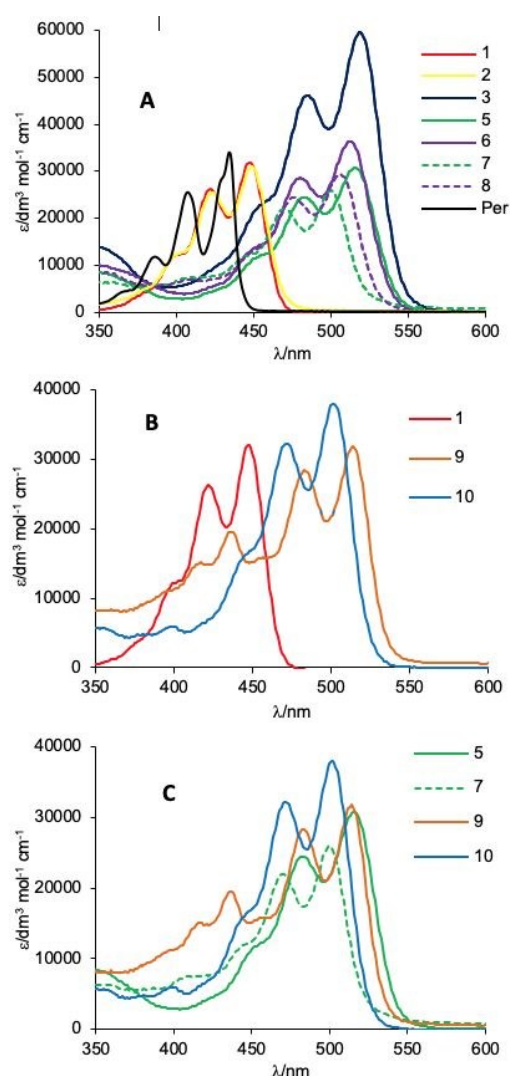


Fig. 5 Absorption spectra recorded in CHCl₃ solution ($\sim 10^{-5}$ M) at room temperature: A) Perylene, HPerPy (**1**) and its Ag and Pd complexes **2–3** and **5–8**; B) HPerPy (**1**) and its Pt complexes **9–10**; C) Comparison plot: Pd^{II} six-membered cycle **5** and Pd^{II} five-membered cycle **7**, Pt^{II} **9**, Pt^{IV} **10**.

Molecular orbital calculations

DFT calculations were performed using B3LYP with LANL2DZ to analyse the absorption spectra of ligand **1**, and the representative complexes **5**, **7**, **9** and **10**. Computational details are given in the Experimental Section. The results are shown in Table 3 and Fig. 6. Some calculated values collected in Table 3 correspond to transitions of low intensity that can be not experimentally observable. Figure 6 depicts only the most intense transitions. Simulated spectra for these compounds are given in Figure S19 in the ESI[†].

For HPerPy (**1**), two intense bands are predicted. The most intense, at 465 nm, is experimentally observed in chloroform solution very close to the calculated value (Table 2), and corresponds to a HOMO → LUMO transition.^{6a,12,13} Both orbitals are centred in the perylene π-system (94 and 91%, respectively). A second peak is expected at 261 nm, composed by different single monoexcitations between π systems of the perylene, in particular between the HOMO and the higher π* empty orbital in Fig. 6 (calculated values for perylene are 442 and 257 nm, respectively).¹³ These two absorptions are characteristic of all the perylene derivatives,^{6a,6b,12,13,17,20} and can be found in all the spectra, although modified in energy. Interestingly, the six-membered-cyclometallated complex [Pd(PerPy)(acac)] (**5**) shows in the calculations a clear red shift to 534 nm of the HOMO → LUMO transition. The analysis of involved orbitals reveals that the observed energy change in this band due to some destabilization of the HOMO and stabilization of the LUMO upon formation of the six-membered metallacycle. The contribution of perylene in the LUMO decreases from 91% to 71% and the participation of the pyridine orbitals increases from 5% to 23%. The HOMO incorporates contribution of the metal orbitals (5%). On the other hand, higher energy bands related with the HOMO are calculated at 274 nm (to π*(Per)) and 337 nm. Experimentally these bands appear at 516, 355 and 270 nm (Table 2). Furthermore, other low intensity transitions are predicted in the visible region.

For the spectra of the five-membered-cyclometallated complexes [M(PerPy)(acac)] (M = Pd (**7**), Pt (**9**)), calculations predict very similar red shifts of the HOMO → LUMO transition to 514 and 519 nm, respectively, whereas the transition at 261 nm in the ligand is red shifted to 273 and 276 nm, respectively. Again, the contribution of perylene in the LUMO decreases from 91% to ~70% and the participation of the pyridine orbitals increases from 5% to 20%. This change alters the wavelength of the former band, but it has little influence in the second one. The calculated values match reasonably those found experimentally: 500 and 246 nm for Pd, 514 and 265 nm for Pt (Table 2). Comparing the features of the bands labelled in Table 3 as MLCT from πd(M) + π(acac) to π*(Per)_{LUMO} for the Pd^{II} and Pt^{II} complexes **7** and **9**, the transition predicted for **9** at 420 nm is assigned to an intense absorption band observed experimentally at 436 nm. However, the absorption of the related medium intensity transition predicted for **7** at 403 nm is

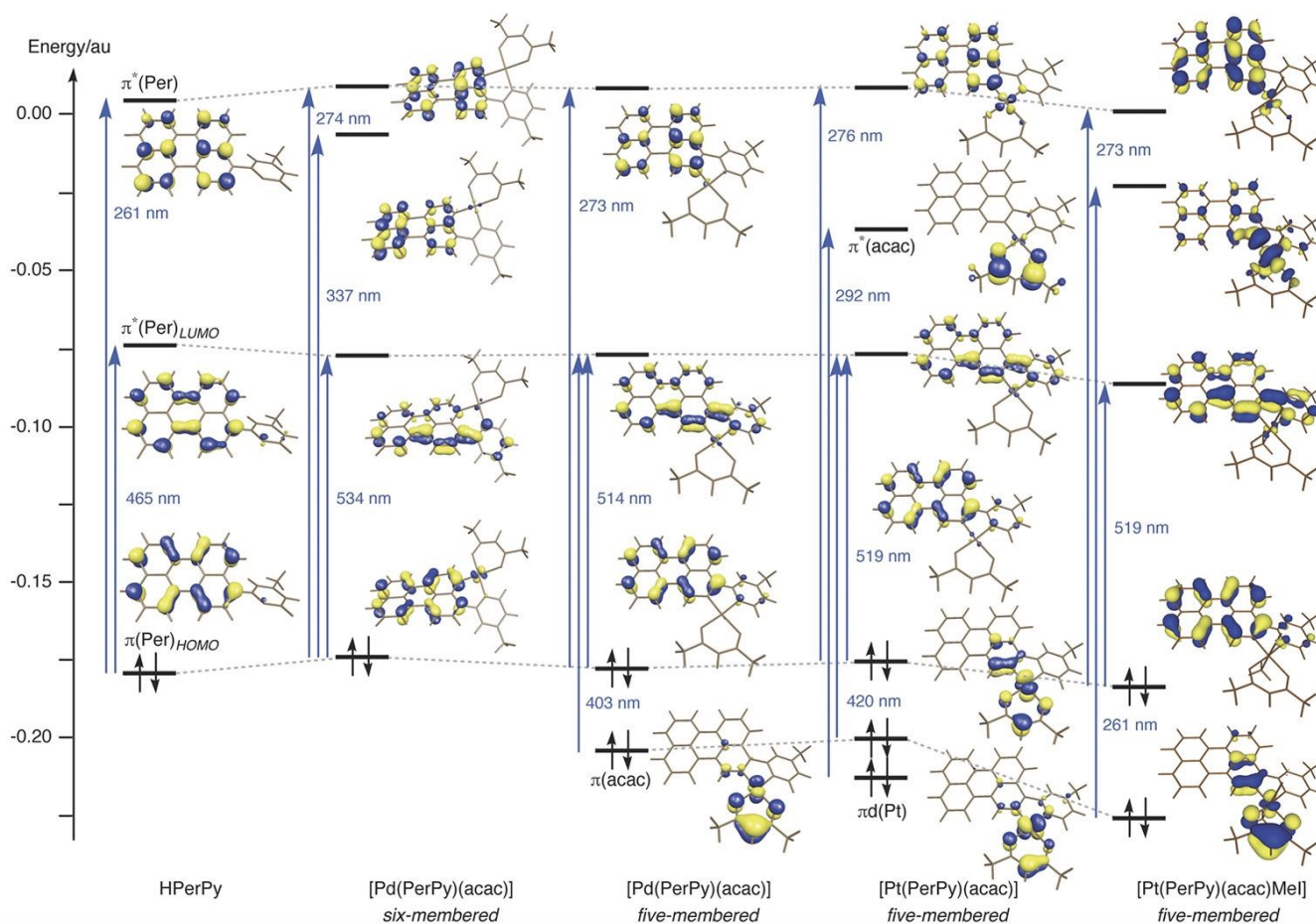
hard to identify in the experimental spectrum. Since the energy and composition of the LUMO hardly change with the metal in this case, the different behaviour has to be ascribed to the changes in energy and composition of the occupied orbitals. For **7**, the filled orbital is centred in the acac fragment, with just poor contribution of the metal (this transition could be named, perhaps more properly, LLCT), whereas for **9** the transition has similar participation from both, the acac and the metal, and has a higher MLCT character.

Finally, the calculated spectrum for the Pt^{IV} five-membered-metallacycle complex [Pt(PerPy)(acac)Me] (**10**) is more dominated by transitions centred in the perylene fragment. In comparison to [Pt(PerPy)(acac)] (**9**), the energy levels are lower in Pt^{IV} than in Pt^{II}, but the composition of molecular orbitals and their relative energies are not different enough to expect large changes, resulting in transitions almost coincident with those of **9** at 519 and 273 nm. Experimentally these bands appear at 502 and 270 nm for Pt^{IV} compound **10** (Table 2). Other transitions that might reflect the decrease of overlapping between Pt^{IV} and the perylene orbitals, due to contraction of the former upon oxidation, are experimentally less significant due to their low intensity or (as for the band calculated at 420 nm for Pt^{II}) to their overlapping with other transitions in the same range associated to perylene.

Table 3. Calculated absorption parameters (wavelengths in nm and their intensities) for the perylenylpyridine derivatives in chloroform solution.^{a,b}

Assignment	HPerPy (1)	six-membered [Pd(PerPy)(acac)] (5)	[Pd(PerPy)(acac)] (7)	five-membered [Pt(PerPy)(acac)] (9)	[Pt(PerPy)(acac)MeI] (10)
Perylene: $\pi(\text{Per}) \rightarrow \pi^*(\text{Per})$	465 (0.69) 261 (0.37) 257 (0.07)	534 (0.64) 337 (0.08) 274 (0.15)	514 (0.66) 273 (0.29) 263 (0.10)	519 (0.61) 276 (0.14) 267 (0.16)	519 (0.65) 336 (0.06) 273 (0.18)
MLCT: $\pi d(\text{M}) + \pi(\text{acac}) \rightarrow \pi^*(\text{Per})_{\text{LUMO}}$	-	388 (0.04)	403 (0.07)	420 (0.14)	-
Perylene, ILCT: $\pi(\text{Per})_{\text{HOMO}} \rightarrow \pi^*(\text{Per,Py})$	-	321 (0.07)	-	321 (0.08)	410 (0.07)
MLCT: $\pi d(\text{M}) + \pi(\text{acac}) \rightarrow \pi^*(\text{Py})$	-	296 (0.02) 275 (0.06)	303 (0.04) 255 (0.05)	300 (0.09) 271 (0.08)	306 (0.06) 275 (0.07) 261 (0.09)
acac: $\pi d(\text{M}) + \pi(\text{acac}) \rightarrow \pi^*(\text{acac})$	-	279 (0.08)	286 (0.08)	292 (0.13)	323 (0.06)

^a Values in bold are represented in Fig 6. ^b A complete assignment of the absorption spectra parameters is available from ESI (Table S4[†]). MLCT = metal-to-ligand charge-transfer. ILCT = interligand charge-transfer.

**Fig. 6.** Schematic representation of main expected transition in the absorption spectra of HPerPy and its complexes.

Luminescence spectra. In the solid state, the emission bands have very low intensity and show a broad maximum that is shifted to lower energy with respect to the solution (from 3200 to 3630 cm^{-1} , for the metal complexes). Specific data are collected in Table S6, and the emission spectra are shown in Figures S22-S23 in the ESI[†].

Much more interesting is the behavior in solution. Luminescence data of the perylenylpyridine ligand **1** and its metallic complexes at room temperature in chloroform are summarized in Table 2. The luminescence spectra are shown in Fig. 7.

The ligand displays an emission in the range 450–550 nm, red-shifted 1360 cm^{-1} compared to perylene. No changes are observed in the silver compound **2**. Palladium and platinum compounds display red-shifted emissions from 500 to 650 nm. Overall, red shifts (maximum of 3150 cm^{-1}) are observed for the emission maxima after formation of metallacycles with HPerPy ligand, depending on the metal fragment. The order is similar to that observed in the absorption spectra: ligand and **2** < platinum(IV) **10** and palladium(II) (five-member cycles) **7** < platinum(II) **9** and palladium(II) (five-member cycles) **8** < palladium(II) (six-member cycle) **3**, **5**–**6**.

The presence of vibronic structure, with a vibrational spacing of $\sim 1200 \text{ cm}^{-1}$ related to the stretching C–C frequency of the polyaromatic system indicates perylene character for the transition. Based on the small Stokes shifts between absorption and emission (maximum of 2110 cm^{-1} in compound **6**), and the short emission lifetimes (in the range 0.023–3.95 ns; most of them are biexponential; Table 2) the luminescence observed can be assigned to π – π^* fluorescence of ligand character. Our calculated electronic spectra also point out to a perylene centred emission modified by the metallic fragment. This is true also for platinacycles for which phosphorescence has been often reported: the emission properties are nearly unaffected in the presence of O_2 , and none phosphorescence can be detected for the complexes even at 77 K (spectra of **5**, **7**, **9**–**10**, in frozen Me-THF, show no additional emission bands; only the vibronic structure is better resolved as defined peaks (See Figure S20 in the ESI[†]). Besides, measurements for platinum compounds **9**–**10** in several solvents with different polarity, show displacement maxima of 290 cm^{-1} , which again suggests fluorescence due to the perylene moiety (See Figure S21 in the ESI[†]).

These results differ from those obtained for the corresponding complexes based on pyrene (pyrenylpyridine). For them, weakly phosphorescent red-emitting species cyclometallated Pt^{II} ($\lambda_{\text{em}} = 680 \text{ nm}$, $\Phi = 0.005$; $\lambda_{\text{em}} = 692 \text{ nm}$, Φ up to 0.0068) were reported.^{24,25} For a cyclometallated Pt^{IV} complex a dual emission has been reported: fluorescence at room temperature, but phosphorescence at 77K or in a rigid media as polystyrene ($\lambda_{\text{em}} = 684 \text{ nm}$, quantum yield too weak to be measured).²⁶ These works confirm that phosphorescence in perylene derivatives is not an easy target because the high and extensive π –delocalization in perylene promotes HOMO and LUMO to be mainly centred in

the perylene moiety, which facilitates fluorescence. Moreover, phosphorescence in cyclometallated Pd^{II} , Pt^{II} and Pt^{IV} is often measured at low temperature (and is strongly temperature-dependent) due to the existence of thermally activated non-radiative states, which prevent luminescence.²⁷

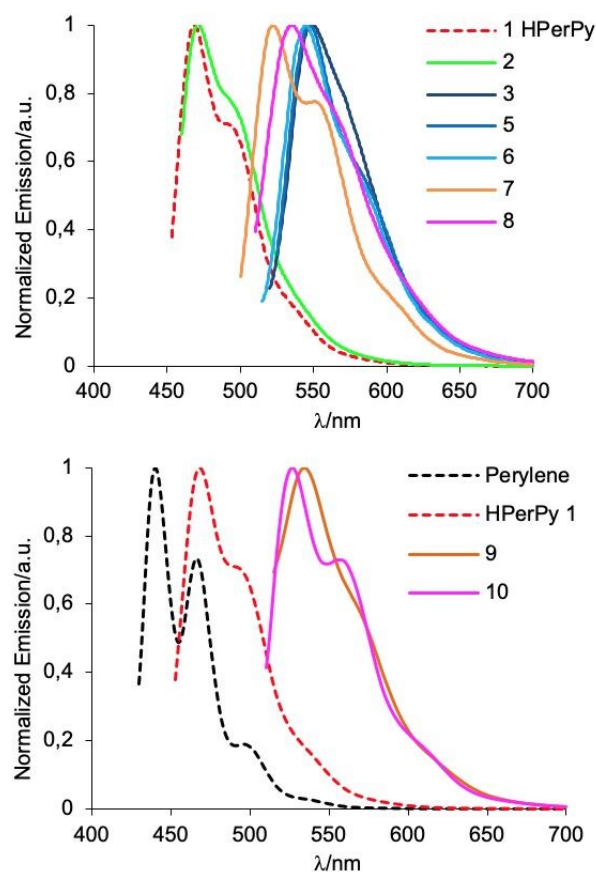


Fig. 7 Emission spectra recorded in CHCl_3 solution (10^{-5} M) at room temperature of HPerPy (**1**) and its complexes, up Ag and Pd; down Pt.

The emission quantum yields of perylenepyridine and its complexes were measured in chloroform at room temperature and the data are summarized in Table 2. The free ligand exhibits a very high quantum yield of 0.82 close to the reported for perylene ($\Phi_{\text{fl}} = 0.92$).²⁸ Silver compound **2** maintains a high quantum yield of 0.78, which confirms that the perylene and the pyridine are weakly coupled, due to the non coplanarity of these fragments in the corresponding X-ray structure. We reported similar results by studying the ligand 3-tetrafluorophenyl-perylene and its complexes.¹²

As shown in the X-ray diffraction studies, metallation forces a fairly planar geometry of the Perylene and the Py components of the PerPy ligand in the five-membered complexes, whereas less coplanar geometry is produced in their six-membered isomers. The experimental result is that the six-membered complexes conserve higher quantum yields than their planar five-membered isomers. For instance, the six-membered

[Pd(PerPy)(acac)] (**5**) quantum yield ($\Phi_{\text{fl}} = 0.47$) is 2-fold that of its five-membered (**7**) isomer ($\Phi_{\text{fl}} = 0.25$). Similar result is observed in the xanthate compounds, with $\Phi_{\text{fl}} = 0.055$, respectively, for the six-membered (**6**) and $\Phi_{\text{fl}} = 0.027$ for the five-membered (**8**) isomers. Interestingly, the acac derivatives are 10-fold more fluorescent than the corresponding xanthate compounds, which confirms a significant influence of the auxiliary ligand. Clearly, the planar five-membered cyclopalladated complexes suffer considerable quenching of the quantum yield compared to the six-membered isomers. The fluorescence quenching associated to planarity has been attributed to a photoinduced intramolecular electron transfer (PET) process induced by the pyridine.^{20,29,30} Our calculations show that metallacycle formation results in a lower participation of the perylene in frontier orbitals (especially in LUMO), by increased percentage of the pyridine and M orbitals.

Substitution of Pd by Pt in the five-membered [M(PerPy)(acac)] complexes (**7** vs. **9**) diminishes 23-fold the quantum yield ($\Phi_{\text{fl}} = 0.011$ for the Pt complex **9**) due to the influence of spin-orbit coupling associated to the heavy atom effect of Pt, inducing a faster S to T intersystem crossing where the level of radiationless d-d transition is lower than that of emissive energy in triplet state, so that T1 is relaxed through thermally non-radiative d-d deactivation processes.¹⁹ A similar result was reported for perylene dimide, where the quantum yields dropped only from 100 to 37 after σ -coordination of a PtCl(PPh₃)₂ fragment (compare with the case of our silver complex), but much more sharply, to 5, upon metalation to a planar 5-membered platinacycle.¹⁹

Unexpectedly, a significant 20-fold enhancement in fluorescence was observed in the platinum(IV) compound **10** ($\Phi_{\text{fl}} = 0.2$), which suggests an attenuation of the quenching process in the platinum(II) complexes.

In summary, quantum yield exhibits a remarkably complex dependence on the different metals, the ancillary ligands, the oxidation state, and the cycle size. The fluorescence quantum yield order found is: five-membered [Pt(PerPy)(acac)] **9** < five-membered palladium(II) **3** < five-membered [Pd(PerPy)(xant)] **8** < six-membered [Pd(PerPy)(xant)] **6** < five-membered platinum(IV) **10**; and five-membered [Pd(PerPy)(acac)] **7** < six-membered [Pd(PerPy)(acac)] **5** < HPerPy **1**, silver complex **2**.

Conclusions

The reaction of 2-(3-perylenyl)-4-methylpyridine (HPerPy) with Pd(OAc)₂ yields five or six-membered metallacycles, depending on the conditions used. However, the reaction with K₂PtCl₄ leads to a five-membered metallacycle.

Six X-ray studies confirm the proposed structures. In our previous studies 6+6 and 6+5 palladacycles were observed, now we have characterized the 5+5 dinuclear palladacycle.

The perylenylpyridine ligand and its silver complex are highly luminescent due to the weak (hence non-disturbing) electronic coupling between perylene and pyridine (they are non-coplanar). In contrast, metallacycle formation dramatically

decreases the luminescence, much more than when the same metal is bonded directly to the perylene core. Five-membered cycles show perylene/metal-coordination-plane and perylene/py arrangements almost coplanar, which may contribute to produce lower fluorescence quantum yield compared to the corresponding non-coplanar six-membered metallacycles. As reported for the related perylene imine metallacycles, the heavy atom Pt^{II} is detrimental for fluorescence compared to Pd^{II}. In contrast, Pt^{IV} reduces the electronic connection with the perylene core and leads to a remarkable enhancement of the emission intensity. The ancillary chelate ligand has also a significant influence, and acac derivatives exhibit a 10-fold intensity enhancement compared to xanthate analogues. This differs with the results found in perylene imine derivatives where the xanthate derivatives were up to 2-fold more luminescent. Phosphorescence, often observed for platinacycles with aryl pyridines, was not observed in our complexes.

Experimental Section

Materials and general methods. All reactions were carried out under dry nitrogen. The solvents were purified according to standard procedures. Literature methods were used to prepare 3-bromoperylene,³¹ 3-perylene boronic ester,²¹ [Ag(PPh₃)(OCIO₃)],³² Pd(OAc)₂,³³ K₂PtCl₄,³⁴ and [Ti(acac)].³⁵ C, H, N analyses were carried out on a Perkin-Elmer 2400 microanalyzer. IR spectra (cm⁻¹) were recorded on a Perkin-Elmer Frontier spectrometer coupled to a Pike GladiATR-210 accessory. ¹H NMR and ³¹P NMR spectra were recorded on Bruker AV-400 or Varian 500 spectrophotometers in CDCl₃ solutions, with chemical shifts referred to TMS (¹H) or 85% H₃PO₄ (³¹P). UV-vis absorption spectra were obtained on a Shimadzu UV-2550 spectrophotometer, in chloroform solution (~ 1 × 10⁻⁵ M). Luminescence data were recorded on a Perkin-Elmer LS-55 luminescence spectrometer, in chloroform (~ 1 × 10⁻⁵ M). Solid state measurements were made using finely ground KBr dispersions of the sample in 5 mm quartz tubes at room temperature. Luminescence quantum yields were obtained at room temperature using the optically dilute method (A < 0.1) in degassed chloroform (quantum yields standard were perylene in ethanol ($\Phi_{\text{fl}} = 0.92$),²⁸ rhodamine 123 in ethanol,³⁶ and rhodamine B in ethanol ($\Phi_{\text{fl}} = 0.70$),³⁷ and cresyl violet in ethanol ($\Phi_{\text{fl}} = 0.54$)³⁸ and using an excitation wavelength of 434, 510 and 488 nm, respectively). The emission lifetime measurements were carried out with a Lifespec-red picosecond fluorescence lifetime spectrometer or with a Halcyone fluorescence spectrometer. The technique used is "Time Correlated Single Photon Counting" (TCSPC). The lifetime data were fitted using mono and double exponential functions.

Computational details. Unrestricted calculations were carried out using the Gaussian09 package.³⁹ The hybrid density function method known as B3LYP was applied.⁴⁰ Effective core potentials (ECP) were used to represent the innermost electrons of the transition atoms (Pd and Pt) and the basis set

of valence double- ζ quality for associated with the pseudopotentials known as LANL2DZ.⁴¹ The basis set for the main group elements was 6-31G* (C, N, O and H).⁴² Solvent effects of chloroform (or other solvents) were taken into account by PCM calculations,⁴³ keeping the geometry optimized for gas phase (single-point calculations). Excited states and absorption spectra were obtained from the time-dependent algorithm implemented in Gaussian09.⁴⁴

Synthesis of 2-(3-perilynyl)-4-methylpyridine (1)

To a solution of 3-perylene boronic ester (0.860 g, 2.27 mmol) in dry THF (90 mL) under nitrogen were added CsF (0.700 g, 4.61 mmol), PdCl₂(dppf) (0.167 g, 0.228 mmol) and 2-bromo-4-methylpyridine (0.258 mL, 2.28 mmol). The mixture was stirred for 85 h at 65°C, then the solvents were distilled off, and the resulting residue was chromatographed (silica gel, hexane/CH₂Cl₂ 1:1 as eluent). A final yellow band was collected using MeOH/CH₂Cl₂ (5%) and the solvent was evaporated to obtain the product as a yellow solid. Yield: 0.413 g (48%). Anal. Calcd. for C₂₆H₁₇N: C, 90.93; H, 4.99; N, 4.08. Found: C, 90.65; H, 5.25; N, 3.90. ¹H-NMR (400 MHz, CDCl₃): δ 8.66 (d, J = 5.0 Hz, 1H, H^A), 8.26 (d, J = 7.9 Hz, 1H), 8.25 – 8.18 (m, 3H), 7.95 (d, J = 8.5 Hz, 1H), 7.71 (d, J = 8.1 Hz, 1H), 7.70 (d, J = 8.2 Hz, 1H), 7.59 (d, J = 7.8 Hz, 1H), 7.50 (td, J = 7.9, 1.8 Hz, 2H), 7.46 (d, J = 7.4 Hz, 1H), 7.43 (d, J = 0.8 Hz, 1H, H^X), 7.17 (dd, J = 5.0, 0.8 Hz, 1H, H^M), 2.47 (s, 3H, CH₃^{PY}).

Synthesis of [Ag(HPerPy)(PPh₃)(OCIO₃)] (2)

To a solution of HPerPy (1) (0.041 g, 0.12 mmol) in CH₂Cl₂ (15 mL) was added Ag(PPh₃)(OCIO₃) (0.057 g, 0.12 mmol). The mixture was stirred in darkness for 4 h. The solvent was evaporated in vacuo and the yellow solid was washed with diethyl ether (2 x 3 mL). Yield: 89 mg (91%). Anal. Calcd. for C₄₄H₃₂AgNPClO₄: C, 74.06; H, 4.52; N, 1.96. Found: C, 74.29; H, 4.26; N, 1.82. ¹H-NMR (400 MHz, CDCl₃): δ 9.03 (d, J = 5.6 Hz, 1H, H^A), 8.01 (t, J = 8.0 Hz, 2H), 7.95 (dd, J = 7.8, 3.4 Hz, 2H), 7.71 (t, J = 8.6 Hz, 1H), 7.66 (d, J = 8.3 Hz, 1H), 7.59 (d, J = 7.7 Hz, 1H), 7.55 – 7.38 (m, 5H), 7.24 – 7.06 (m, 10H), 7.02 – 6.90 (m, 6H), 2.53 (s, 3H, CH₃^{PY}). ³¹P{¹H} NMR (122 MHz, CDCl₃): δ 14.11 (¹J_{Ag-P} = 712 Hz). IR (KBr, cm⁻¹): 1096, 1048 v(Cl-O).

Synthesis of (μ -OOCCH₃)₂[Pd(PerPy)]₂-six-membered (3)

To a suspension of 1 (0.168 g, 0.49 mmol) in dry methanol (50 mL) was added Pd(OAc)₂ (0.110 g, 0.49 mmol) and the mixture was stirred at room temperature for 15 h. The red solid was filtered and then stirred with toluene (10 mL) for 5 h. The precipitate was collected and dried under vacuum. Yield: 274 mg (56%). Anal. Calcd. for C₅₆H₃₈N₂O₄Pd₂: C, 66.21; H, 3.77; N, 2.76. Found: C, 66.55; H, 4.03; N, 2.54. ¹H-NMR (400 MHz, CDCl₃): δ 8.16 (d, J = 7.0 Hz, 1H), 8.08 (d, J = 6.0 Hz, 1H, H^A), 8.00 (d, J = 7.4 Hz, 1H), 7.71 – 7.66 (m, 3H), 7.63 (d, J = 7.9 Hz, 1H), 7.48 (t, J = 7.8 Hz, 1H), 7.43 (t, J = 7.8 Hz, 1H), 7.28 (d, J = 7.0 Hz, 1H), 7.19 (d, J = 1.3 Hz, 1H, H^X), 7.03 (d, J = 8.0 Hz, 1H), 6.52 (dd, J = 6.1, 1.4 Hz, 1H, H^M), 2.06 (s, 3H, CH₃^{PY}), 1.81 (s, 3H, CH₃COO-).

Synthesis of (μ -OOCCH₃)₂[Pd(PerPy)]₂-five-membered (4)

To a suspension of 1 (0.109 g, 0.32 mmol) in acetic acid (8 mL) was added Pd(OAc)₂ (0.072 g, 0.32 mmol) and the mixture was stirred at 70 °C for 6 h. The solvent was evaporated to dryness and the residue was stirred with toluene (10 mL) for 5 h at room temperature. The red precipitate was collected and dried under vacuum. It is a mixture of two isomers: 66% of 5+5 isomer and 34% of 5+6 isomer. Yield: 127 mg (78%). ¹H-NMR (400 MHz, CDCl₃) major product: δ 8.20 (d, J = 6.7, 1.0 Hz, 1H, H^A), 8.11 (d, J = 7.7 Hz, 1H), 8.09 (d, J = 7.7 Hz, 1H), 7.85 (d, J = 6.4 Hz, 1H), 7.84 (s, 1H, H^I), 7.75 (d, J = 8.0 Hz, 1H), 7.74 (d, J = 8.0 Hz, 1H), 7.67 (d, J = 8.4 Hz, 1H), 7.54 (t, J = 7.4 Hz, 1H), 7.52 (t, J = 7.5 Hz, 1H), 7.39 (d, J = 7.6 Hz, 2H), 7.01 (d, J = 1.1 Hz, 1H, H^X), 5.91 (dd, J = 5.7, 1.0 Hz, 1H, H^M), 2.43 (s, 3H, CH₃^{PY}), 1.47 (s, 3H, CH₃COO-).

Synthesis of [Pd(PerPy)(acac)]-six-membered (5)

To a solution of 3 (0.056 g, 0.055 mmol) in dry CH₂Cl₂ (10 mL) was added a solution of KOH in methanol (378 μ L, 0.19 mmol, 0.5 M) and acetylacetone (22 μ L, 0.21 mmol). After 24 h of stirring at room temperature, the solvent was evaporated to dryness. The residue was solved in CH₂Cl₂ and the solution was filtered through a Kieselguhr filter and concentrated in vacuo to a small volume. The addition of diethyl ether produced a red precipitate, which was collected on a frit and washed with diethyl ether (2 x 3 mL). Yield: 57 mg (95%). Anal. Calcd. for C₃₁H₂₃NO₂Pd: C, 67.95; H, 4.23; N, 2.56. Found: C, 68.03; H, 4.34; N, 2.72. ¹H-NMR (400 MHz, CDCl₃): δ 9.07 (d, J = 6.1 Hz, 1H, H^A), 8.23 (d, J = 7.4 Hz, 1H), 8.21 (t, J = 7.7 Hz, 2H), 8.08 (d, J = 8.0 Hz, 1H), 8.02 (d, J = 8.2 Hz, 1H), 7.87 (d, J = 8.0 Hz, 1H), 7.73 (d, J = 1.7 Hz, 1H, H^X), 7.70 (d, J = 8.0 Hz, 1H), 7.63 (d, J = 8.0 Hz, 1H), 7.48 (t, J = 7.8 Hz, 1H), 7.47 (t, J = 7.8 Hz, 1H), 7.10 (dd, J = 6.2, 1.8 Hz, 1H, H^M), 5.39 (s, 1H, CH^{acac}), 2.44 (s, 3H, CH₃^{PY}), 2.05 (s, 3H, CH₃^{acac}), 2.04 (s, 3H, CH₃^{acac}).

Synthesis of [Pd(PerPy)(S₂COMe)]-six-membered (6)

To a solution of 3 (0.040 g, 0.040 mmol) in dry CH₂Cl₂ (10 mL) was added a solution of KOH in methanol (316 μ L, 0.16 mmol, 0.5 M) and CS₂ (96 μ L, 1.6 mmol). Workup as above. Yield: 34 mg (77%). Anal. Calcd. for C₂₈H₁₉NOPdS₂: C, 60.48; H, 3.44; N, 2.52. Found: C, 60.11; H, 3.61; N, 2.64. ¹H-NMR (400 MHz, CDCl₃): δ 8.91 (d, J = 5.9 Hz, 1H, H^A), 8.24 (d, J = 7.5 Hz, 1H), 8.23 (d, J = 8.1 Hz, 1H), 8.20 (d, J = 7.5 Hz, 1H), 8.03 (d, J = 8.1 Hz, 1H), 7.96 (d, J = 7.8 Hz, 1H), 7.78 (s, 1H, H^X), 7.72 (d, J = 8.1 Hz, 1H), 7.69 (d, J = 7.7 Hz, 1H), 7.65 (d, J = 8.1 Hz, 1H), 7.51 (t, J = 8.0 Hz, 1H), 7.47 (d, J = 7.7 Hz, 1H), 7.06 (d, J = 5.9 Hz, 1H, H^M), 4.24 (s, 3H, OCH₃), 2.45 (s, 3H, CH₃^{PY}).

Synthesis of [Pd(PerPy)(acac)]-five-membered (7)

The method was the same as 5 but with the use of 4. Yield: 55 mg (85%). Anal. Calcd. for C₃₁H₂₃NO₂Pd: C, 67.95; H, 4.23; N, 2.56. Found: C, 67.69; H, 3.99; N, 2.83. ¹H-NMR (400 MHz, CDCl₃): δ 8.74 (d, J = 5.7 Hz, 1H, H^A), 8.60 (s, 1H, H^I), 8.36 (d, J = 7.5 Hz, 1H), 8.27 (d, J = 8.5 Hz, 1H), 8.23 (d, J = 7.5 Hz, 1H), 8.17 (d, J = 7.5 Hz, 1H), 7.97 (s, 1H, H^X), 7.71 (d, J = 8.1 Hz, 2H), 7.61 – 7.43 (m, 3H), 6.99 (d, J = 5.5 Hz, 1H, H^M), 5.46 (s, 1H, CH^{acac}), 2.51 (s, 3H, CH₃^{PY}), 2.24 (s, 3H, CH₃^{acac}), 2.10 (s, 3H, CH₃^{acac}).

Synthesis of [Pd(PerPy)(S₂COMe)]-five-membered (8)

The method was the same as **6** but with the use of **4**. Yield: 30 mg (46%). Anal. Calcd. for C₂₈H₁₉NOPdS₂: C, 60.48; H, 3.44; N, 2.52. Found: C, 60.58; H, 3.64; N, 2.74. ¹H-NMR (400 MHz, CDCl₃): δ 8.38 (d, J = 5.6 Hz, 1H, H^A), 8.27 – 8.19 (m, 3H), 8.16 (d, J = 7.6 Hz, 1H), 8.04 (s, 1H, H^X), 7.96 (s, 1H, H¹), 7.69 (d, J = 8.1 Hz, 2H), 7.56 – 7.39 (m, 3H), 6.96 (d, J = 5.5 Hz, 1H, H^M), 4.32 (s, 3H, OCH₃), 2.49 (s, 3H, CH₃^{Py}).

Synthesis of [Pt(PerPy)(acac)]-five-membered (9)

To a suspension of HPerPy (**1**) (0.251 g, 0.731 mmol) in 2-ethoxyethanol (10 mL) was added K₂PtCl₄ (0.101 g, 0.244 mmol) in water (5 mL). The mixture was heated at reflux for 22 h. After being cooled to room temperature, 30 mL of water was added to the mixture. The red-orange precipitate was filtered and washed with water (2 x 5 mL) and diethyl ether (2 x 5 mL). To the suspension of the precipitate in CH₂Cl₂ (30 mL) was added Ti(acac) (0.078 g, 0.256 mmol) and the mixture stirred at room temperature for 5 h. After then the solution was filtered and evaporated to dryness. The resulting crude product was purified by column chromatography (silica gel, CH₂Cl₂). An orange solid was obtained. Yield: 118 mg (25%). Anal. Calcd. for C₃₁H₂₃NO₂Pt: C, 58.49; H, 3.64; N, 2.20. Found: C, 58.86; H, 3.89; N, 2.41. ¹H-NMR (500 MHz, CDCl₃): δ 8.95 (d, ³J_{HPt} = 39.8 Hz, J = 6.0 Hz, 1H, H^A), 8.61 (s, ³J_{HPt} = 38.5, 1H, H¹), 8.38 (d, J = 7.4 Hz, 1H), 8.29 (d, J = 8.5 Hz, 1H), 8.23 (d, J = 7.4 Hz, 1H), 8.17 (d, J = 7.4 Hz, 1H), 7.99 (d, J = 0.6 Hz, 1H, H^X), 7.70 (d, J = 7.7 Hz, 2H), 7.61 – 7.42 (m, 3H), 6.93 (dd, J = 5.9, 0.6 Hz, 2H, H^M), 5.53 (s, 1H, CH^{acac}), 2.51 (s, 3H, CH₃^{Py}), 2.14 (s, 3H, CH₃^{acac}), 2.04 (s, 3H, CH₃^{acac}).

Synthesis of [Pt(PerPy)(acac)MeI]-five-membered (10)

To a suspension of **2** (0.032 g, 0.050 mmol) in dry acetone (10 mL) was added MeI (0.14 mL, 2.22 mmol). The mixture was stirred at room temperature for 48 h, and then the solvent was evaporated under reduce pressure. The light orange solid was washed with diethyl ether (2 x 5 mL). Yield: 37 mg (94%). Anal. Calcd. for C₃₂H₂₆IINO₂Pt: C, 49.37; H, 3.37; N, 1.80. Found: C, 49.47; H, 3.23; N, 1.82. ¹H-NMR (400 MHz, CDCl₃): δ 9.10 (d, ³J_{HPt} = 33.2 Hz, J = 6.1 Hz, 1H, H^A), 8.64 (s, ³J_{HPt} = 29.1 Hz, 1H, H¹), 8.42 (dd, J = 7.7, 1.0 Hz, 1H), 8.35 (d, J = 8.3 Hz, 1H), 8.27

(dd, J = 7.7, 1.0 Hz, 1H), 8.24 (dd, J = 7.0, 0.6 Hz, 1H), 8.20 (d, J = 1.2 Hz, 1H, H^X), 7.77 (d, J = 7.7 Hz, 1H), 7.75 (d, J = 7.9 Hz, 1H), 7.63 (dd, J = 8.5, 7.6 Hz, 1H), 7.59 – 7.47 (m, 2H), 7.11 (dd, J = 6.1, 1.2 Hz, 1H, H^M), 5.62 (s, 1H, CH^{acac}), 2.64 (s, 3H, CH₃^{Py}), 2.30 (s, 3H, CH₃^{acac}), 2.24 (s, 3H, CH₃^{acac}), 1.42 (s, ³J_{HPt} = 65.9 Hz, 3H, CH₃).

X-ray Crystal Structure Analysis. Single crystals of compounds **2**, **4**, **5**, **8**, **9**, and **10** suitable for X-ray diffraction studies were obtained from slow diffusion of hexane into a tetrahydrofuran solution of **2** (at -20 °C), **5** or **8** (at room temperature); from slow diffusion of diethyl ether into a tetrahydrofuran solution of **4** (at room temperature), into a chloroform solution of **9** (at room temperature) or into a dichloromethane solution of **10**. Relevant crystallographic details are given in the ESI Table S2†. Crystals were mounted in glass fibers, and diffraction measurements were made using an Oxford Diffraction Supernova diffractometer equipped with an Atlas CCD area detector. Data collection was performed with Mo-K_α radiation (λ = 0.71073 Å). Data integration, scaling and empirical absorption corrections were carried out using the CrysAlis Pro software package.⁴⁵ The structure was solved using direct methods and refined by Full-Matrix-Least-Squares against F² with SHELX⁴⁶ in OLEX2.⁴⁷ The non-hydrogen atoms were refined anisotropically and hydrogen atoms were placed at idealized positions and refined using the riding model. The molecular structures were created with Olex2 and Mercury.⁴⁸ In the structure of compound **2** the perchlorate anion was found to be disordered in two positions keeping O3 as common pivotal atom. The two alternate positions refined to occupation factors of 0.6 and 0.4. In the structure of compound **4** several peaks were found which could be due to a disordered molecule of THF. Since it could not be satisfactorily modelled, the corresponding electron density was treated with the Solvent Mask tool implemented in Olex2. Crystallographic data (excluding structure factors) for the structures reported in this paper have been deposited with the Cambridge Crystallographic Data Centre as Supplementary publications with the deposition numbers CCDC-2015584 for **2**, CCDC-2015585 for **4**, CCDC-2015586 for **5**, CCDC-2015587 for **8**, CCDC-2015588 for **9**, and CCDC-2015589 for **10**. Copies of the data can be obtained free of charge on application to the CCDC, 12 Union Road, Cambridge CB2 1EZ, U.K. [Fax: (internat.) + 44-1223/336-033; Email: deposit@ccdc.cam.ac.uk].

Conflicts of interest

There are no conflicts to declare.

Acknowledgements

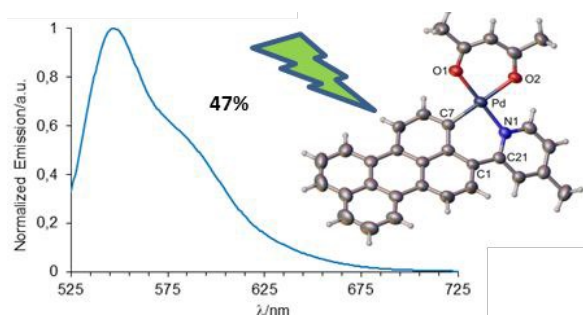
We gratefully acknowledge the Ministerio de Economía y Competitividad (Project CTQ2017-89217-P) and the Junta de Castilla y León (Project VA038G18) for financial support. Allocation of computer facilities at IQTCUB is also acknowledged. The measurements were carried out in part in the Laboratory of Instrumental Techniques (LTI) Research Facilities, Universidad de Valladolid.

Notes and references

- ¹ H. Zollinger, *Color Chemistry*, Wiley-VCH, Weinheim, 3rd edn, 2003.
- ² See for example: (a) C. Li and H. Wonneberger, *Adv Mater.*, 2012, **24**, 613; (b) E. Kozma and M. Catellani, *Dyes Pigm.*, 2013, **98**, 160; (c) M. R. Wasielewski, *J. Org. Chem.*, 2006, **71**, 5051; (d) T. Weil, T. Vosch, J. Hofkens, K. Peneva and K. Müllen, *Angew. Chem., Int. Ed.*, 2010, **49**, 9068; (e) Y. Lin, Y. Wang, J. Wang, J. Hou, Y. Li, D. Zhu and X. Zhan, *Adv. Mater.* 2014, **26**, 5137; (f) C. Huang, S. Barlow and S. R. Marder, *J. Org. Chem.*, 2011, **76**, 2386; (g) Y. Li, T. Liu, H. Liu, M. Tian and Y. Li, *Acc. Chem. Res.*, 2014, **47**, 1186; (h) L. Schmidt-Mende, A. Fechtenkötter, K. Müllen, E. Moons, R. Friend and J. D. MacKenzie, *Science*, 2011, **293**, 1119.
- ³ (a) F. Würthner, C. Thalacker, S. Diele and C. Tschierske, *Chem. – Eur. J.*, 2001, **7**, 2245; (b) Z. Chen, U. Baumeister, C. Tschierske and F. Würthner, *Chem. – Eur. J.*, 2007, **13**, 450; (c) Z. Chen, V. Stepanenko, V. Dehm, P. Prins, L. D. A. Siebbeles, J. Seibt, P. Marquetand, V. Engel and F. Würthner, *Chem. – Eur. J.*, 2007, **13**, 2245.
- ⁴ F. Würthner, T. E. Kaiser and C. R. Saha-Möller, *Angew. Chem., Int. Ed.*, 2011, **50**, 3376.
- ⁵ (a) Z. An, J. Yu, S. C. Jones, S. Barlow, S. Yoo, B. Domercq, P. Prins, L. D. A. Siebbeles, B. Kippelen and S. R. Marder, *Adv. Mater.*, 2005, **17**, 2580; (b) C. Domínguez, M. J. Baena, S. Coco and P. Espinet, *Dyes Pigm.*, 2017, **140**, 375.
- ⁶ See for example: (a) S. Lentijo, J. A. Miguel and P. Espinet, *Organometallics*, 2011, **30**, 1059; (b) S. Lentijo, J. A. Miguel and P. Espinet, *Dalton Trans.*, 2011, **40**, 7602; (c) K. Yamada, H. Mori, T. Sugaya, M. Tadokoro, J. Maeba, K. Nozaki and M. Haga, *Dalton Trans.*, 2019, **48**, 15212.
- ⁷ (a) J. Dupont, M. Pfeffer, *Palladacycles*, ed., Wiley-VCH, Weinheim, 2008; (b) R. C. Evans, P. Douglas and C. J. Winscom, *Coord. Chem. Rev.*, 2006, **250**, 2093; (c) I. Omae, *J. Organomet. Chem.*, 2017, **848**, 184.
- ⁸ (a) M. Ghedini, I. Aiello, M. La Deda and A. Grisolia, *Chem. Commun.*, 2003, 2198; (b) P. K. Chow, C. Ma, W.-P. To, G. S. M. Tong, S.-L. Lai, S. C. F. Kui, W.-M. Kwok and C.-M. Che, *Angew. Chem. Int. Ed.*, 2013, **52**, 11775; (c) M. Micutz, M. Ilis, T. Staicu, F. Dumitrascu, I. Pasuk, Y. Molard, T. Roisnel and V. Cîrcu, *Dalton Trans.*, 2014, **43**, 1151; (d) P.-K. Chow, W.-P. To, K.-H. Low and C.-M. Che, *Chem. Asian J.*, 2014, **9**, 534; (e) C. Xu, H. M. Li, Z. Q. Xiao, Z. Q. Wang, S. F. Tang, B. M. Ji, X. Q. Hao and M. P. Song, *Dalton Trans.*, 2014, **43**, 10235; (f) C. Xu, Z. Q. Wang, X. E. Yuan, X. Han, Z. Q. Xiao, W. J. Fu, B. M. Ji, X. Q. Hao and M. P. Song, *J. Organomet. Chem.*, 2015, **777**, 1.
- ⁹ (a) J. Kalinowski, V. Fattori, M. Cocchi and J. A. G. Williams, *Coord. Chem. Rev.*, 2011, **255**, 2401; (b) S. Huo, J. Carroll and D. A. K. Vezzu, *Asian J. Org. Chem.*, 2015, **4**, 1210; (c) A. K. W. Chan, M. Ng, Y. C. Wong, M. Y. Chan, W. T. Wong and V.W. W. Yam, *J. Am. Chem. Soc.*, 2017, **139**, 10750; (d) D. N. Kozhevnikov, V. N. Kozhevnikov, M. Z. Shafikov, A. M. Prokhorov, D. W. Bruce and J. A. G. Williams, *Inorg. Chem.*, 2011, **50**, 3804; (e) A. Petrenko, K. Leitonas, D. Volyniuk, G. V. Baryshnikov, S. Belyakov, B. F. Minaev, H. Ågren, H. Durgaryan, J. V. Gražulevičius and P. Arsenyan, *Dalton Trans.*, 2020, **49**, 3393.
- ¹⁰ (a) F. Juliá, D. Bautista, J. M. Fernández-Hernández and P. González-Herrero, *Chem. Sci.*, 2014, **5**, 1875; (b) A. Vivancos, D. Poveda, A. Muñoz, J. Moreno, D. Bautista and P. González-Herrero, *Dalton Trans.*, 2019, **48**, 14367.
- ¹¹ F. Castellano, *Dalton Trans.*, 2012, **41**, 8493 and references cited therein.
- ¹² S. Lentijo, G. Aullón, J. A. Miguel and P. Espinet, *Dalton Trans.*, 2013, **42**, 6353.
- ¹³ S. Lentijo, J. E. Expósito, G. Aullón, J. A. Miguel and P. Espinet, *Dalton Trans.*, 2014, **43**, 10885.
- ¹⁴ (a) A.A. Rachford, S. Goeb and F.N. Castellano, *J. Am. Chem. Soc.* 2008, **130**, 2766; (b) A.A. Rachford, S. Goeb, R. Ziesel and F.N. Castellano, *Inorg. Chem.* 2008, **47**, 4348.
- ¹⁵ J. E. Yarnell, A. Chakraborty, M. Myahkostupov, K. M. Wright and F. N. Castellano, *Dalton Trans.*, 2018, **47**, 15071.
- ¹⁶ M. Schulze, A. Steffen, and F. Würthner, *Angew. Chem., Int. Ed.*, 2015, **54**, 1570-1573.
- ¹⁷ S. Lentijo, J. A. Miguel and P. Espinet, *Inorg. Chem.*, 2010, **49**, 9169.
- ¹⁸ H. Weissman, E. Shirman, T. Ben-Moshe, R. Cohen, G. Leitus, L.J.W. Shimon and B. Rybtchinski, *Inorg. Chem.*, 2007, **46**, 4790.
- ¹⁹ J. E. Yarnell, I. Davydenko, P. V. Dorovatovskii, V. N. Khrustalev, T. V. Timofeeva, F. N. Castellano, S. R. Marder, C. Risko and Stephen Barlow, *J. Phys. Chem. C*, 2018, **122**, 13848.
- ²⁰ J. E. Expósito, M. Álvarez-Paíno, G. Aullón, J. A. Miguel and P. Espinet, *Dalton Trans.*, 2015, **44**, 16164.
- ²¹ Y. Avlasevich and K. Müllen, *J. Org. Chem.* 2007, **72**, 10243.
- ²² Z. Li, P. Cui, C. Wang, S. Kilina, and W. Sun, *J. Phys. Chem. C* 2014, **118**, 28764.
- ²³ (a) A. Pidcock, R. E. Richards and L. M. Venanzi, *J. Chem. Soc. A*, 1966, 1707; (b) T. G. Appleton, H. C. Clark and L. E. Manzer, *Coord. Chem. Rev.*, 1973, **10**, 335.
- ²⁴ W. Wu, W. Wu, S. Ji, H. Guo and J. Zhao, *Eur. J. Inorg. Chem.*, 2010, 4470.
- ²⁵ (a) N. Su, F. Meng, J. Chen, Y. Wang, H. Tan, S. Su and W. Zhu, *Dyes Pigm.*, 2016, **128**, 68-74; (b) N. Su, F. Meng, P. Wang, X. Liu, M. Zhu, W. Zhu, S. Su and J. Yu, *Dyes Pigm.*, 2017, **138**, 162.
- ²⁶ N. Giménez, E. Lalinde, R. Lara, and M. T. Moreno, *Chem. Eur. J.*, 2019, **25**, 5514.
- ²⁷ (a) F. Barigelletti, D. Sandrini, M. Maestri, V. Balzani, A. von Zelewsky, L. Chassot, P. Jolliet and U. Maeder, *Inorg. Chem.*, 1988, **27**, 3644; (b) T. Sajoto, P. I. Djurovich, A. B. Tamayo, J. Oxgaard, W. A. Goddard III and M. E. Thompson, *J. Am. Chem. Soc.*, 2009, **131**, 9813.
- ²⁸ M. Montalti, A. Credi, L. Prodi and M. T. Gandolfini, *Handbook of Photochemistry*, 3rd ed.; CRC Pres LLC: Boca Raton, FL, 2005.
- ²⁹ (a) A. P. De Silva and R. A. D. D. Rupasinghe, *Chem. Commun.*, 1985, 1669; (b) B. P. de Silva, H. Q. N. Lgunaratne, T. L. Gunnlangsson, A. J. M. Unzley, C. P. McCoy, J. T. Rademacher and T. E. Rice, *Chem. Rev.*, 1997, **97**, 1515; (c) R. Martínez-Mañez and F. Sancenón, *Chem. Rev.*, 2003, **103**, 4419.
- ³⁰ (a) A. W. Czarnik, *Acc. Chem. Res.* 1994, **27**, 302; (b) H. Wang, D. Wang, Q. Wang, X. Li and C. A. Schalley, *Org. Biomol. Chem.*, 2010, **8**, 1017; (c) N. I. Georgiev, A. R. Sakr, A. R. and V. B. Bojinov, *Dyes Pigm.* 2011, **91**, 332; (d) X. J. Liu, N. Zhang, J. Zhou, T. J. Chang, C. L. Fang and D. H. Shangquan, *Analyst*, 2013, **138**, 901; (e) S. Malkondu, *Tetrahedron*, 2014, **70**, 5580; (f) H.

- Wang, Y. Lang, H. Wang, J. Lou, H. Guo and X. Li, *Tetrahedron*, 2014, **70**, 1997.
- E. Pidcock, L. Rodriguez-Monge, R. Taylor, J. van de Streek and P. A. Wood, *J. Appl. Crystallogr.*, 2008, **41**, 466.
- ³¹ (a) R. H. Mitchell, Y. H. Lai and R. V. Williams, *J. Org. Chem.*, 1979, **44**, 4733. (b) R. Lapuyade, J. Pereyre and P. C. R. Garrigues, *Acad. Sci. Ser. II*, 1986, **303**, 903.
- ³² F. A. Cotton, L. R. Falvello, R. Usón, J. Forniés, M. Tomas, J. M. Casas and I. Ara, *Inorg. Chem.*, 1987, **26**, 1366.
- ³³ T. A. Stephenson, S. M. Morehouse, A. R. Powell, J. P. Heffer and J. G. Wilkinson, *J. Chem. Soc.*, 1965, 3632.
- ³⁴ R. N. Keller, *Inorg. Synth.*, 1946, **2**, 247.
- ³⁵ E. C. Taylor; G. H. Hawks and A. Mckillop, *J. Am. Chem. Soc.*, 1968, **90**, 2421.
- ³⁶ A.H. Abdelrahman, M. A. Abdelrahman and M. K. Elbadawy, *Natural Science*, 2013, **5**, 1183.
- ³⁷ F. López-Arbeloa, P. Ruiz-Ojeda and I. López-Arbeloa, *J. Luminesc.*, 1989, **44**, 105.
- ³⁸ D. Magde, J. H. Brannon, T. L. Cremers and J. Olmsted, *J. Phys. Chem.*, 1979, **83**, 696.
- ³⁹ M. J. Frisch, G. W. Trucks, H. B. Schlegel, G. E. Scuseria, M. A. Robb, J. R. Cheeseman, G. Scalmani, V. Barone, B. Mennucci, G. A. Petersson, H. Nakatsuji, M. Caricato, X. Li, H. P. Hratchian, A. F. Izmaylov, J. Bloino, G. Zheng, J. L. Sonnenberg, M. Hada, M. Ehara, K. Toyota, R. Fukuda, J. Hasegawa, M. Ishida, T. Nakajima, Y. Honda, O. Kitao, H. Nakai, T. Vreven, J. A. Montgomery, Jr., J. E. Peralta, F. Ogliaro, M. Bearpark, J. J. Heyd, E. Brothers, K. N. Kudin, V. N. Staroverov, T. Keith, R. Kobayashi, J. Normand, K. Raghavachari, A. Rendell, J. C. Burant, S. S. Iyengar, J. Tomasi, M. Cossi, N. Rega, J. M. Millam, M. Klene, J. E. Knox, J. B. Cross, V. Bakken, C. Adamo, J. Jaramillo, R. Gomperts, R. E. Stratmann, O. Yazyev, A. J. Austin, R. Cammi, C. Pomelli, J. W. Ochterski, R. L. Martin, K. Morokuma, V. G. Zakrzewski, G. A. Voth, P. Salvador, J. J. Dannenberg, S. Dapprich, A. D. Daniels, O. Farkas, J. B. Foresman, J. V. Ortiz, J. Cioslowski and D. J. Fox, *Gaussian 09 (Revision B.1)*; Gaussian Inc.: Wallingford CT 2010.
- ⁴⁰ (a) A. D. Becke, *J. Chem. Phys.*, 1993, **98**, 5648; (b) C. Lee, W. Yang and R. G. Parr, *Phys. Rev. B*, 1988, **37**, 785.
- ⁴¹ P. J. Hay and W. R. Wadt, *J. Chem. Phys.*, 1985, **82**, 299.
- ⁴² (a) P. C. Hariharan and J. A. Pople, *Theoret. Chim. Acta*, 1973, **28**, 213; (b) M. M. Francl, W. J. Pietro, W. J. Hehre, J. S. Binkley, M. S. Gordon, D. J. DeFrees and J. A. Pople, *J. Chem. Phys.*, 1982, **77**, 3654.
- ⁴³ (a) J. Tomasi, M. Persico, *Chem. Rev.*, 1994, **94**, 2027; (b) C. Amovilla, V. Barone, R. Cammi, E. Cancès, M. Cossi, B. Mennucci, C. S. Pomelli and J. Tomasi, *Adv. Quantum Chem.*, 1998, **32**, 227.
- ⁴⁴ M. E. Casida, C. Jamorski, K. C. Casida and D. R. Salahub, *J. Chem. Phys.*, 1998, **108**, 4439.
- ⁴⁵ v. CrysAlisPro-Data Collection and Integration Software, Agilent Technologies UK Ltd, Oxford, UK, 2011.
- ⁴⁶ G. Sheldrick, *Acta Crystallogr., Sect. A: Found. Crystallogr.*, 2008, **64**, 112–122.
- ⁴⁷ O. V. Dolomanov, L. J. Bourhis, R. J. Gildea, J. A. K. Howard and H. Puschmann, *J. Appl. Cryst.*, 2009, **42**, 339.
- ⁴⁸ C. F. Macrae, I. J. Bruno, J. A. Chisholm, P. R. Edgington, P. McCabe,

Table of Contents



Perylenylpyridine cyclometallated complexes exhibit fluorescence with quantum yields from 1.1 to 47% depending on the metal, the oxidation state, the auxiliary ligand and the size of the metallacycle (5 or 6).